# Microstructure functions for a model of statistically inhomogeneous random media

J. Quintanilla* and S. Torquato †
*Princeton Materials Institute and Department of Civil Engineering and Operations Research, Princeton University, Princeton, New Jersey 08544*
(Received 8 August 1996)

We propose a model for statistically inhomogeneous two-phase random media, including functionally graded materials, consisting of inhomogeneous fully penetrable (Poisson distributed) spheres. This model can be constructed for any specified variation of volume fraction and permits one to represent and evaluate certain $n$-point correlation functions that statistically characterize the microstructure for this model. Unlike the case of statistically homogeneous media, the microstructure functions depend upon the absolute positions of their arguments. However, as with homogeneous random media, this microstructural information will be useful in obtaining rigorous estimates of the effective properties of such systems. [S1063-651X(98)08601-2]

PACS number(s): 05.20.−y, 61.43.Hv, 61.43.Gt

## I. INTRODUCTION

Much progress has been made in recent years in characterizing the microstructure of statistically homogeneous two-phase random media via a variety of $n$-point correlation functions [1–3]. For ergodic ensembles, the $n$-point correlation functions are translationally invariant, that is, statistical homogeneity is implied [4], and hence one can equate ensemble averages with volume averages in the infinite-volume limit. This microstructural information is fundamental in rigorously determining the effective transport, electromagnetic and mechanical properties of ergodic two-phase random media [3,5–10].

Significantly less research has been devoted to the study of *statistically inhomogeneous* two-phase media. In such instances, ergodicity is lost; that is, one cannot equate ensemble and volume averages. One simple example of such a medium is any two-phase system that is defined on a finite region. However, as we will describe in Sec. II, defining a two-phase medium on an infinite region does not preclude statistical inhomogeneity. Examples of statistically inhomogeneous, two-phase media include porous media with spatially variable fluid permeability [11], composites in which the heterogeneity length scale is not much smaller than the macroscopic size of the sample, distributions of galaxies [12], and functionally graded materials [13–18].

We define $\phi_i(\mathbf{x})$ to be the volume fraction of phase $i$ at a point $\mathbf{x}$, so that $\phi_1(\mathbf{x})+\phi_2(\mathbf{x})=1$ for all $\mathbf{x}$. Although most applications permit $\phi_1(\mathbf{x})$ to vary in only one direction, it can be chosen to be any function in principle. Simple models of statistically inhomogenous media include layered media, so that $\phi_1(x)$ is a step function. For macroscopically rectangular systems, a more complicated grade that has been previously studied is [17]

$$\phi_1(x)=\left(\frac{x_2-x}{x_2-x_1}\right)^{\alpha}, \tag{1}$$

where $\alpha$ is specified and $x_1$ and $x_2$ are the $x$ coordinates of the left and right edges of the system, respectively. Another variation of the volume fraction is given by

$$\phi_1(x)=a_0+a_1x+a_2x^2, \tag{2}$$

where the coefficients are chosen so that $0\leqslant\phi_1(x)\leqslant 1$ within the system. However, a specific microstructural model is not typically presented that obeys these or other specified grades in volume fraction, and hence higher-order microstructural information in the form of $n$-point correlation functions has heretofore not been obtained.

Following the development of the study of the microstructure and properties of homogeneous random media [3], we propose a microstructural model for particulate, statistically inhomogeneous two-phase random media in this paper. This model is a two-phase system consisting of an *inhomogeneous distribution of fully penetrable spheres* in space whose particle density obeys *any specified variation in volume fraction*. The space exterior to the spheres is called phase 1, and phase 2 is the space occupied by the spheres. This inhomogeneous model is nontrivial in that cluster formation naturally arises and it permits significantly more complicated microstructures than the aforementioned layered models. Four two-dimensional realizations of this model with different grades are shown in Fig. 1.

Explicitly defining this model permits a quantitative characterization of its microstructure, and we will use the theory of nonstationary Poisson process to develop analytical expressions for various microstructure functions that have been evaluated previously for homogeneous models [3]. These functions include the canonical $n$-point microstructure function $H_n$ [2], the nearest-neighbor functions $E$ and $H$ [19], and the lineal-path function $L$ [20]. Definitions and prior analytical expressions for these functions are presented before their evaluation for inhomogeneous fully penetrable spheres. Unlike the homogeneous case, *these microstructure functions will depend on the absolute positions of their arguments*, as discussed in Sec. IV. This statistical character-

*Present address: Department of Mathematics, University of North Texas, Denton, TX 76203. Electronic address: johnq@cardinal.math.unt.edu

†Author to whom correspondence should be addressed. Electronic address: torquato@matter.princeton.edu

 

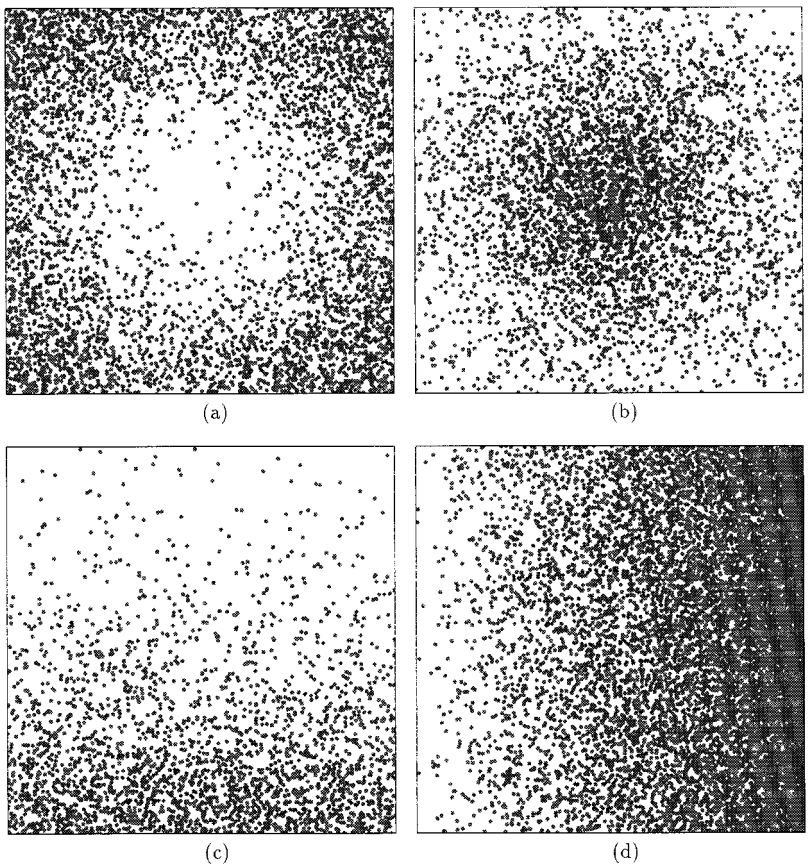


FIG. 1. Four realizations of statistically inhomogeneous fully penetrable disks. System (a) may be thought of as arising from a centrifugal field, while system (b) can be viewed as a system in an ''anticentrifugal'' field. System (c) is one under a constant gravitational field in the vertical direction, whereas system (d) has a linear grade in the volume fraction in the horizontal direction. The density functions of systems (a)–(d) are given by Eqs. (7)–(10), respectively, with parameters that are given in the text.

ization of the microstructure for two-phase random media will undoubtedly be fundamental in the study of the effective properties.

In Sec. II, we describe the mathematical underpinnings of systems of inhomogeneous fully penetrable spheres. We also describe how such systems can be generated by computer simulation. In Sec. III, we discuss previous analytical results for the microstructure functions considered in this paper. These functions are evaluated for inhomogeneous fully penetrable spheres in Sec. IV.

## II. DEFINITION OF INHOMOGENEOUS FULLY PENETRABLE SPHERES

In this section, we provide the mathematical basis for systems of inhomogeneous fully penetrable spheres. Although based upon the theory of general Poisson processes and measure theory [21], we will not use the full abstractions of this theory to describe these systems. We then describe how realizations of inhomogeneous fully penetrable spheres may be generated by computer simulations.

### A. Mathematical basis

We will consider $D$-dimensional space $\mathbb{R}^D$ as our measurable space. We also assume that $\nu$ is a *measure* on $\mathbb{R}^D$, so that the measure $\nu B$ of any measurable set $B$ with respect to $\nu$ is given by

$$\nu B = \int_B \rho(\mathbf{x}) d\mathbf{x} \tag{3}$$

for some function $\rho$ on $\mathbb{R}^D$. When $\rho(\mathbf{x})=1$ for all $\mathbf{x}$, the measure $\nu$ is ordinary Lebesgue measure and hence $\nu B$ is simply the volume of $B$. Condition (3) is satisfied if $\nu$ is absolutely continuous to Lebesgue measure [21].

A *general Poisson process* $\mathcal{N}$ with intensity measure $\nu$ is defined to be a point process that satisfies the following two properties [22]: (i) The number of points in a bounded Lebesgue set $B$ has any Poisson distribution with mean $\nu B$, that is, for $m=0,1,2,\ldots,$

$$\Pr(\mathcal{N}(B)=m)=\frac{(\nu B)^m}{m!}e^{-\nu B}. \tag{4}$$

(ii) For all $n\geqslant 2$, the random variables $\mathcal{N}(A_1),\ldots,\mathcal{N}(A_n)$ are independent whenever the Lebesgue sets $A_1,\ldots,A_n$ are pairwise disjoint.

The density $\rho(\mathbf{x})$ is called the *density function* of $\mathcal{N}$; this function will be used often in this paper. It is important to note that if $\rho(\mathbf{x})=\rho$, a constant, then a general Poisson process reduces to an ordinary Poisson process with number density (or intensity) $\rho$. However, even if $\rho(\mathbf{x})$ is not con-

stant, it has an appealing intuitive interpretation: $\rho(\mathbf{x})d\mathbf{x}$ is the probability that there is a point of $\mathcal{N}$ in an infinitesimal region $d\mathbf{x}$ about $\mathbf{x}$.

We notice from condition (i) that the probability that a region $B$ contains no points of $\mathcal{N}$ is

$$\Pr(\mathcal{N}(B)=0)=e^{-\nu B}=\exp\left[-\int_B \rho(\mathbf{x})d\mathbf{x}\right]. \tag{5}$$

This calculation of the *exclusion probability* for $B$ will be used repeatedly for different sets $B$ in the calculations of Sec. IV.

We also notice that this general framework can be used to define systems on a *finite* region $\mathcal{R}$ by choosing the intensity function to be the restriction of $\rho$ to $\mathcal{R}$, that is,

$$\rho_{\mathcal{R}}(\mathbf{x})=\begin{cases}\rho(\mathbf{x}), & \mathbf{x}\in\mathcal{R}\\ 0 \quad \text{otherwise.}\end{cases} \tag{6}$$

The microstructure functions for such finite systems are then calculated by using $\rho_{\mathcal{R}}$ in place of $\rho$.

### B. Simulation of inhomogeneous fully penetrable spheres

Constructing realizations of general Poisson processes can be easily done in two stages if the density function $\rho(\mathbf{x})$ is bounded on $\mathbb{R}^D$ [22], say, $\rho(\mathbf{x})\leq\rho^*$. First, a Poisson process of density $\rho^*$ is simulated. Second, the resulting point pattern is thinned. Each point $\mathbf{x}$, independently of the other points, is kept with probability $\rho(\mathbf{x})/\rho^*$ or deleted with probability $1-\rho(\mathbf{x})/\rho^*$. The resulting point pattern is a general Poisson process with intensity function $\rho(\mathbf{x})$. This construction may be enhanced by partitioning $\mathbb{R}^D$ into regions in which $\rho(\mathbf{x})$ does not vary significantly. Finally, we place spheres of common radius $R$ on the points of $\mathcal{N}$ to construct a realization of inhomogeneous fully penetrable spheres.

Four examples of the density function are given as

$$\rho(x,y)=C\left(\frac{r\lambda L}{R}\right)^2, \tag{7}$$

$$\rho(x,y)=\frac{C}{R^2}\exp\left(-\frac{r\lambda}{L}\right), \tag{8}$$

$$\rho(x,y)=\frac{C}{R^2}\exp\left(-\frac{y\lambda}{L}\right), \tag{9}$$

$$\rho(x,y)=\frac{C}{R^2}\ln\left(\frac{[1+\epsilon]\lambda}{[1+\epsilon]L-x}\right), \tag{10}$$

respectively. Here $r$ is the distance from a fixed point (say the center of the system), $C$ is a multiplicative factor, $L$ is the length scale of the entire system, $\lambda$ is the length scale of the grade in volume fraction, and $\epsilon$ is very small. For all of these systems, the origin is placed at the lower-left corner. As discussed above, the value of the density function $\rho(\mathbf{x})$ at a given point $\mathbf{x}$ is directly correlated to the average density of centers around $\mathbf{x}$. The systems generated by these density functions may be thought of as arising from special external fields. System (a) [Eq. (7)] may be thought of as arising from a centrifugal field, while system (b) [Eq. (8)] can be viewed as a system in an ''anticentrifugal'' field. System (c) [Eq. (9)] is one under a constant gravitational field in the vertical direction, whereas, as we will show in Sec. IV, system (d) [Eq. (10)] has a linear grade in the volume fraction in the horizontal direction when $C=1/\pi$, given by

$$\phi_1(x)\approx\frac{(1+\epsilon)L-x}{(1+\epsilon)\lambda}. \tag{11}$$

Other systems with different grades in volume fractions can also be constructed with different choices of the density function $\rho(\mathbf{x})$.

Note that there are *three* length scales associated with these systems: the size of the particles $R$, the size of the region $L$, and the length scale $\lambda$ of the variation of $\rho(x,y)$. Even if the region is taken to be infinite, there will still be two length scales for these systems, namely, $R$ and $\lambda$. This is in contrast to homogeneous two-phase random media on infinite domains, which possess only the length scale of the particles. We again note that statistically inhomogeneous systems are not ergodic and hence ensemble averages cannot be equated with volume averages.

In Fig. 1 we present realizations of inhomogeneous fully penetrable disks with density functions given by Eqs. (7)–(10). Although only two-dimensional realizations are presented, the simulation procedure may be used in higher dimensions as well. For all four systems (a)–(d), the size of the particles is $R=1$ and the macroscopic system size is $L=200$. We also use the following parameters [for systems (a)–(d), respectively] to generate Fig. 1:

$$C=0.8,\lambda=1, \tag{12}$$

$$C=0.6,\lambda=5, \tag{13}$$

$$C=0.3,\lambda=4, \tag{14}$$

$$C=1/\pi,\lambda=L. \tag{15}$$

We also notice that the maximum volume fraction of phase 2 in system (d) is $\phi_2\approx 1$ along the right edge; but the maximum particle volume fraction for system (c) is roughly $\phi_2\approx 0.6$ on the bottom edge.

We see in these figures that even the concept of volume fraction has lost its simplicity: the probability that a point lies in a sphere is dependent on the absolute location of the point. In fact, all of the usual microstructure functions will depend on the absolute positions of the arguments. Nonetheless, the general theory of Poisson processes can be employed to characterize the microstructure of inhomogeneous fully penetrable spheres.

Examples of inhomogeneous media that may be modeled similarly to systems (b) and (d) are described in [23] and [24], respectively. In [23], the authors consider a cylindrical *in situ* Al-$Al_3Ni$ functionally graded material in which the volume fraction of $Al_3Ni$ increases with radial distance. These authors then measured the Young modulus and internal friction of the composite. In [24], these authors considered the production of Ti-Al/$TiB_2$ composites. The transitions between layers for these materials were found to be approximately linear. We refer the reader to [13–18] for fur-

ther discussion of the different grades in volume fraction and properties that have been considered in functionally graded materials.

## III. REVIEW OF THEORETICAL RESULTS FOR MICROSTRUCTURE FUNCTIONS

In this section, we define the canonical $n$-point microstructure function $H_n$, the generic $n$-particle probability density function $\rho_n$, the $n$-point phase-1 probability function $S_n$, the nearest-neighbor functions $E$ and $H$, and the lineal-path function $L$. We also review analytical expressions, obtained by previous researchers, for these functions. In Sec. IV, we will evaluate these functions for inhomogeneous fully penetrable spheres.

### A. Canonical $n$-point microstructure function

We begin to quantify the microstructure of *statistically inhomogeneous* suspensions of spheres, including inhomogeneous fully penetrable spheres, by considering the canonical $n$-point microstructure function $H_n(\mathbf{x}^m;\mathbf{x}^{p-m};\mathbf{r}^q)$ (where $m \leqslant p$ and $p+q=n$), introduced and studied by Torquato [2] for equal-sized spheres. This formalism was later generalized to treat spheres with a polydispersivity in size [25]. As discussed in the introduction, this function has been used in certain rigorous bounds on the effective properties of two-phase random media [3,5–10].

This function is defined for all systems of suspensions of interacting, correlated spheres, including models that require some degree of particle penetrability. [Thus fully penetrable (spatially uncorrelated) spheres are a special case.] To permit this generality, principles from statistical mechanics were employed. We assume that there are $N$ distinguishable spheres that are placed into a volume $V$ and thus consider a statistically inhomogenous system. We define

$$P_N(\mathbf{r}_1, \ldots, \mathbf{r}_N) \equiv P_N(\mathbf{r}^N) \tag{16}$$

to be the probability density function of the $N$ particle centers; that is, the quantity $P_N(\mathbf{r}^N)d\mathbf{r}^N$ gives the probability of finding the center of sphere $i$ in a volume element $d\mathbf{r}_i$ about $\mathbf{r}_i$ for all $i=1, \ldots, N$. From $P_N$, the specific $n$-particle probability density function is then defined to be

$$P_n(\mathbf{r}^n) = \int d\mathbf{r}_{n+1} \ldots d\mathbf{r}_N P_N(\mathbf{r}^N) \tag{17}$$

and the generic $n$-particle probability density function is defined by

$$\rho_n(\mathbf{r}^n) = \frac{N!}{(N-n)!} P_n(\mathbf{r}^n). \tag{18}$$

The quantity $\rho_n(\mathbf{r}^n)d\mathbf{r}^n$ is the probability of finding any sphere center in $d\mathbf{r}_1$ about $\mathbf{r}_1$, another sphere center in $d\mathbf{r}_2$ about $\mathbf{r}_2$, ..., and another sphere center in $d\mathbf{r}_n$ about $\mathbf{r}_n$. For statistically homogeneous systems,

$$\rho_n(\mathbf{r}_1, \ldots, \mathbf{r}_n) = \rho_n(\mathbf{r}_1+\mathbf{y}, \ldots, \mathbf{r}_n+\mathbf{y}) \tag{19}$$

for any vector $\mathbf{y}$, by definition. As a consequence, for statistically homogeneous systems, any of the $n$ points (say, $\mathbf{r}_1$) can be fixed and $\rho_n$ can be expressed as a function of the relative displacements to this fixed point. Mathematically,

$$\rho_n(\mathbf{r}_1, \ldots, \mathbf{r}_n) = \rho_n(\mathbf{r}_{12}, \ldots, \mathbf{r}_{1n}), \tag{20}$$

where $\mathbf{r}_{ij} = \mathbf{r}_j - \mathbf{r}_i$. A simple corollary is that $\rho_1(\mathbf{r}_1) = \rho$, where $\rho$ is the constant number density of spheres. On the other hand, the $\rho_n$ will depend on the absolute position for inhomogeneous fully penetrable spheres; for example, $\rho_1(\mathbf{r}_1) = \rho(\mathbf{r}_1)$, the intensity function defined in Sec. II.

Using this notation, we now define the canonical $n$-point microstructure function. We start by studying the probability $G_n(\mathbf{x}^p;\mathbf{r}^q)d\mathbf{r}^q$ of simultaneously finding $q$ particle centers with configuration $\mathbf{r}^q$ and $p$ ''test spheres'' with respective centers $\mathbf{x}^p$ and radii $a_1, \ldots, a_p$ that contain no particle centers. For $a_i > R$, this is equivalent to test spheres with radii $b_i = a_i - R$ that lie completely outside of the particles. Although the $G_n$ are dependent on the values of the $a_i$, we suppress this dependence in our notation. We notice that

$$G_n(\varnothing, \mathbf{r}^n) = \rho_n(\mathbf{r}^n), \tag{21}$$

the generic $n$-particle probability density function. When $a_i = R$ for all $i$, we define

$$G_n(\mathbf{x}^n;\varnothing) = S_n(\mathbf{x}^n) \tag{22}$$

to be the $n$-point probability function for phase 1. Clearly, $S_1(\mathbf{x}) = \phi_1(\mathbf{x})$, the volume fraction of phase 1 at $\mathbf{x}$.

Torquato [2] showed that $G_n$ for statistically inhomogeneous media can be expressed as

$$G_n(\mathbf{x}^p;\mathbf{r}^q) = \frac{N!}{(N-q)!} \int \prod_{i=1}^{p} \mathcal{I}(\mathbf{x}_i, a_i) P_N(\mathbf{r}^N) d\mathbf{r}_{q+1} \cdots d\mathbf{r}_N, \tag{23}$$

where

$$\mathcal{I}(\mathbf{x};a_i) = \begin{cases} 1, & x \in \mathcal{T}_i \\ 0 & \text{otherwise} \end{cases} \tag{24}$$

and

$$\mathcal{T}_i = \{\mathbf{x}: |\mathbf{x}-\mathbf{r}_j| > a_i \quad \text{for all} \quad j=1, \ldots, N\}. \tag{25}$$

From these definitions,

$$\begin{aligned} \mathcal{I}(\mathbf{x};a_i) &= \prod_{j=1}^{N} [1 - m(y_j;a_i)] \\ &= 1 - \sum_{j=1}^{N} m(y_j;a_i) + \sum_{j<k}^{N} m(y_j;a_i) m(y_k;a_i) \cdots, \end{aligned} \tag{26}$$

where $y_j = |\mathbf{x}-\mathbf{r}_j|$ and

$$m(y;a) = \begin{cases} 1, & y \leqslant a \\ 0, & y > a. \end{cases} \tag{27}$$

Torquato [2] derived both a Kirkwood-Salsburg series representation and a Mayer representation for the $G_n$. We give the latter here and refer the reader to Ref. [2] for the former. He found that

$$G_n(\mathbf{x}^p;\mathbf{r}^q)=\sum_{s=0}^{\infty}(-1)^s G_{n,s}(\mathbf{x}^p;\mathbf{r}^q), \tag{28}$$

where

$$G_{n,0}(\mathbf{x}^p;\mathbf{r}^q)=\rho_q(\mathbf{r}^q)\prod_{k=1}^{p}\prod_{l=1}^{q}e(y_{kl};a_k) \tag{29}$$

for $s=0$ and

$$G_{n,s}(\mathbf{x}^p;\mathbf{r}^q)=\frac{1}{s!}\prod_{k=1}^{p}\prod_{l=1}^{q}e(y_{kl};a_k)\int\rho_{q+s}(\mathbf{r}^{q+s})\times\prod_{j=q+1}^{q+s}\left[1-\prod_{i=1}^{p}e(y_{ij};a_i)\right]d\mathbf{r}_{q+1}\cdots d\mathbf{r}_{q+s} \tag{30}$$

for $s\geqslant 1$. In these expressions $y_{ij}=|\mathbf{x}_i-\mathbf{r}_j|$ and

$$e(y;a)=1-m(y;a). \tag{31}$$

By differentiating Eq. (23) with respect to $a_1,\ldots,a_m$, where $m\leqslant p$, Torquato [2] arrived at the definition of the canonical $n$-point correlation function for statistically inhomogeneous media:

$$H_n(\mathbf{x}^m;\mathbf{x}^{p-m};\mathbf{r}^q)=(-1)^m\frac{\partial}{\partial a_1}\cdots\frac{\partial}{\partial a_m}G_n(\mathbf{x}^p;\mathbf{r}^q), \tag{32}$$

which simplifies as

$$H_n(\mathbf{x}^m;\mathbf{x}^{p-m};\mathbf{r}^q)=\frac{N!}{(N-q)!}\int\left[\prod_{i=1}^{m}\mathcal{M}(\mathbf{x}_i;a_i)\right]\times\left[\prod_{i=m+1}^{p}\mathcal{I}(\mathbf{x}_i,a_i)\right]\times P_N(\mathbf{r}^N)d\mathbf{r}_{q+1}\cdots d\mathbf{r}_N, \tag{33}$$

where

$$\mathcal{M}(\mathbf{x};a_i)=-\frac{\partial\mathcal{I}(\mathbf{x};a_i)}{\partial a_i}=\sum_{j=1}^{N}\delta(a_i-y_j)-\sum_{j<k}^{N}\delta(a_i-y_j)m(y_k;a_i)-\sum_{j<k}^{N}\delta(a_i-y_k)m(y_j;a_i)\cdots \tag{34}$$

and $\delta$ is the Dirac delta function. Again, the $H_n$ are dependent on the values of $a_1,\ldots,a_p$, but we suppress this dependence in our notation. Physically, $\mathcal{M}$ may be thought of as the indicator function of the surface of $\mathcal{T}_i$. Therefore, when $a_i=R$ for all $i$, $H_n(\mathbf{x}^m;\mathbf{x}^{p-m};\mathbf{r}^q)$ may be thought of as the correlation function associated with finding $q$ particle centers with configuration $\mathbf{r}^q$, $p-m$ points $\mathbf{x}^{p-m}$ that lie outside of the particles, and $m$ points $\mathbf{x}^m$ that lie on the surface of the particles. Such microstructural information is known to occur in bounds on the effective properties of two-phase random media [3,5–10].

### B. Nearest-neighbor microstructure functions

Closely related to the $S_n$ are the exclusion probabilities $E_V(\mathbf{x};z)$ and $E_P(\mathbf{x};z)$. The function $E_V(\mathbf{x};z)$ is the probability that the sphere $V_1(\mathbf{x};z)$ of radius $z$ centered at a point $\mathbf{x}$ in the void phase contains no particle centers, while $E_P(\mathbf{x};z)$ is the probability that the sphere contains no other particle centers given that $\mathbf{x}$ is a particle center. For homogeneous and inhomogeneous fully penetrable spheres, these probabilities are identical and will be referred to as $E(\mathbf{x};z)$. Clearly, $E(\mathbf{x};0)=1$ and $E(\mathbf{x};R)=\phi_1(\mathbf{x})$.

The nearest-neighbor distribution function (more accurately, probability density function) is defined from $E$ by

$$H(\mathbf{x};z)=-\frac{\partial E(\mathbf{x};z)}{\partial z}. \tag{35}$$

We notice that these functions are also special cases of the canonical $n$-point microstructure function $H_n$, defined in Sec. III A. If $a_1=z$, then

$$H(\mathbf{x};z)=H_1(\mathbf{x};\varnothing;\varnothing) \tag{36}$$

and

$$E(\mathbf{x};z)=H_1(\varnothing;\mathbf{x};\varnothing). \tag{37}$$

### C. Lineal-path function

The final microstructure function considered in this paper is the lineal-path function $L^{(i)}(z)$, which is the probability that a line segment of length $z$ lies entirely in phase $i$. This microstructure function has been obtained experimentally for sandstone [26] and magnetic gels [27]. For three-dimensional systems, $L^{(i)}(z)$ is also equivalent to the area fraction of phase $i$ measured from the projected image of a three-dimensional slice of thickness $z$ onto a plane [20], a quantity of long-standing interest in stereology [28].

Lu and Torquato [20] showed that, for general systems of spheres,

$$L(z)=1+\sum_{s=1}^{\infty}\frac{(-1)^s}{s!}\int\rho_s(\mathbf{r}^s)\prod_{j=1}^{s}\hat{m}(\mathbf{x}-\mathbf{r}_j;z)d\mathbf{r}_j, \tag{38}$$

where

$$\hat{m}(\mathbf{x};z)=\begin{cases}1, & \mathbf{x}\in\Omega_E(z)\\ 0 & \text{otherwise}\end{cases} \tag{39}$$

and $\Omega_E(z)$ is the exclusion region consisting of all points within the radius $R$ of the line of length $z$. This series expansion for $L(z)$ was obtained by using the same logic as in the derivation of Mayer expansion of $G_n$, and indeed may be

thought of as a special case of $H_n$ with $\hat{m}$ replacing the step function $m$, defined by Eq. (27).

## IV. EVALUATION OF MICROSTRUCTURE FUNCTIONS FOR INHOMOGENEOUS FULLY PENETRABLE SPHERES

In the preceding section, we discussed definitions and theoretical expressions of various microstructure functions. We will now evaluate these functions for inhomogeneous fully penetrable spheres. We find that we obtain identical results for the microstructure functions by using two different methods: the formalism of Sec. III and the exclusion probability (5) of Sec. II. To illustrate our methodology, we also will evaluate and graph these functions for the linear-grade model (d) in Fig. 1. The other systems of Fig. 1 may be treated in a similar fashion, but we do not present these results here since the salient features are brought out well by model (d).

### A. Canonical $n$-point microstructure function

As shown in Eqs. (28) and (32), the canonical $n$-point microstructure function $H_n$ can be obtained as a series in terms of the $n$-particle probability density functions $\rho_s$ for $s \geq q$. For inhomogeneous fully penetrable spheres, this function is clearly given by

$$\rho_s(\mathbf{r}^s) = \rho(\mathbf{r}_1)\cdots\rho(\mathbf{r}_s), \tag{40}$$

and for homogeneous fully penetrable spheres (that is, the underlying Poisson process is spatially stationary)

$$\rho_s(\mathbf{r}^s) = \rho^s, \tag{41}$$

a constant.

For homogeneous fully penetrable spheres, Torquato [2] substituted Eq. (41) into Eq. (28) and found that

$$G_n(\mathbf{x}^p;\mathbf{r}^q) = \rho^q \exp[-\rho V_p(\mathbf{x}^p;a^p)] \prod_{k=1}^{p}\prod_{l=1}^{q} e(y_{kl};a_k). \tag{42}$$

In this expression, $V_p(\mathbf{x}^p;a^p)$ is the union volume of $p$ spheres of radii $a^p \equiv a_1, \ldots, a_p$ centered at $\mathbf{x}_1, \ldots, \mathbf{x}_p$, respectively. Recall that we suppress the dependence of the $G_n$ on the distances $a_i$ in our notation.

Differentiating Eq. (42), the canonical $n$-point correlation function for homogeneous fully penetrable spheres is

$$\begin{aligned} H_n(\mathbf{x}^m;\mathbf{x}^{p-m};\mathbf{r}^q) = {} & (-1)^m \rho^q \exp[-\rho V_p(\mathbf{x}^p;a^p)] \\ & \times \frac{\partial}{\partial a_1}\cdots\frac{\partial}{\partial a_m}\prod_{l=1}^{q}\prod_{k=1}^{p} e(y_{kl};a_k) \\ & + (-1)^m \rho^q \prod_{l=1}^{q}\prod_{k=1}^{p} e(y_{kl};a_k) \\ & \times \frac{\partial}{\partial a_1}\cdots\frac{\partial}{\partial a_m}\exp[-\rho V_p(\mathbf{x}^p;a^p)]. \end{aligned} \tag{43}$$

The expansion (28) can also be evaluated for inhomogeneous fully penetrable spheres with density function $\rho(\mathbf{x})$. After substituting Eq. (40) into Eq. (28) and simplifying, we conclude that

$$\begin{aligned} G_n(\mathbf{x}^p;\mathbf{r}^q) = {} & \rho(\mathbf{r}_1)\cdots\rho(\mathbf{r}_q) \\ & \times \exp\left[-\int_{V_p(\mathbf{x}^p;a^p)} \rho(\mathbf{r})\,d\mathbf{r}\right] \prod_{k=1}^{p}\prod_{l=1}^{q} e(y_{kl};a_k). \end{aligned} \tag{44}$$

Notice that this reduces to Eq. (42) in the special case that $\rho(\mathbf{x})$ is constant.

The expression (44) can also be obtained by using the properties of a nonstationary Poisson process. The $q$ particle centers will have configuration $\mathbf{r}^q$ about $d\mathbf{r}^q$ with probability $\rho(\mathbf{r}_1)\cdots\rho(\mathbf{r}_q)d\mathbf{r}^q$. The probability that $V_p(\mathbf{x}^p;a^p)$ is empty of centers is precisely the exponential term of Eq. (44) in light of Eq. (5). Since these events are independent if the $q$ particle centers do not lie within $V_p(\mathbf{x}^p;a^p)$, we finally obtain Eq. (44).

We also can obtain $H_n$ by inserting Eq. (44) into Eq. (32). We obtain Eq. (43) for inhomogeneous fully penetrable spheres from Eq. (43) with the replacements

$$\rho^q \to \rho(\mathbf{r}_1)\cdots\rho(\mathbf{r}_q), \tag{45}$$

$$\rho V_p(\mathbf{x}^p;a^p) \to \int_{V_p(\mathbf{x}^p;a^p)} \rho(\mathbf{r})\,d\mathbf{r}. \tag{46}$$

### B. Microstructure functions derived from $H_n$

As noted in Eqs. (21) and (22), the $n$-point functions $\rho_n$ and $S_n$ can be obtained from the $H_n$. Using Eq. (44), we see that

$$\rho_n(\mathbf{r}^n) = \rho(\mathbf{r}_1)\cdots\rho(\mathbf{r}_n), \tag{47}$$

as expected, and

$$S_n(\mathbf{x}^n) = \exp\left[-\int_{V_n(\mathbf{x}^n;R)} \rho(\mathbf{r})\,d\mathbf{r}\right], \tag{48}$$

where $V_n(\mathbf{x}^n;R)$ is the union of $n$ spheres with common radius $R$ centered at $\mathbf{x}^n$. In particular,

$$S_1(\mathbf{x}) = \exp\left[-\int_{V_1(\mathbf{x};R)} \rho(\mathbf{r})\,d\mathbf{r}\right]. \tag{49}$$

We see explicitly that, when $\rho(\mathbf{r})$ is not constant, even the concept of volume fraction is dependent on spatial location.

We notice that computing $S_n(\mathbf{x}^n)$ is prohibitively difficult for general $\rho(\mathbf{x})$ due to the complexity of the right-hand side of Eq. (48). However, we can accurately approximate $S_n$ under the assumption that the variation in $\rho$ occurs over a much longer length scale than the size of the spheres. Suppose the region $V_n(\mathbf{x}^n;R)$ can be written as

$$V_n(\mathbf{x}^n;R) = \bigcup_{i=1}^{k} A_i, \tag{50}$$

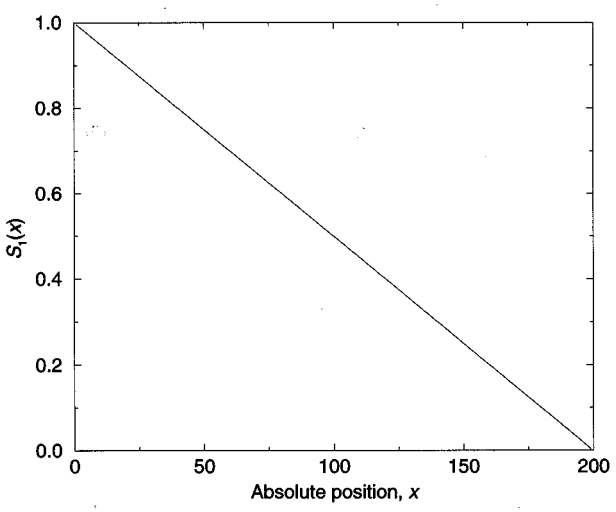


FIG. 2. Microstructure function $\phi_1(x)=S_1(x)$ (that is, the grade in volume fraction) for system (d) of Fig. 1, calculated from Eq. (49). The grade in volume fraction is approximately given by $\phi_1(x)=1-x/L$. The origin of the system is placed in the lower-left corner.

where each $A_i$ is connected and $A_i \cap A_j = \varnothing$ for $i \neq j$. For example, for $n=3$ with $|\mathbf{x}_{12}|<2R$, $|\mathbf{x}_{13}|>2R$, and $|\mathbf{x}_{23}|>2R$, we could set $A_1=V_2(\mathbf{x}_1,\mathbf{x}_2;R)$ and $A_2=V_1(\mathbf{x}_3;R)$; finer decompositions can also be considered. Using Eq. (50), the $S_n$ can be approximated by

$$V_n(\mathbf{x}^n) \approx \exp\left[-\sum_{i=1}^{k} \rho(\mathbf{y}_i)\,\mathrm{vol}(A_i)\right], \tag{51}$$

where $\mathbf{y}_i$ is contained in $A_i$ and $\mathrm{vol}(A_i)$ is the volume of $A_i$.

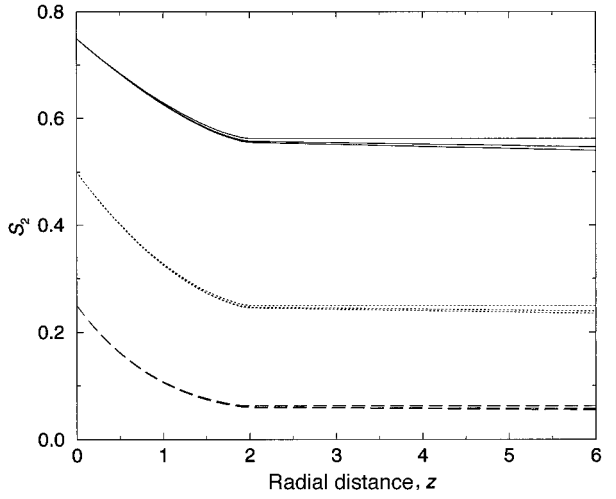


FIG. 3. Two-point probability function $S_2(\mathbf{x}_1,\mathbf{x}_2)$ versus radial distance $z=|\mathbf{x}_2-\mathbf{x}_1|$ for system (d) of Fig. 1. The $x$ coordinate of $\mathbf{x}_1$ is chosen to be 50 (solid lines), 100 (dotted lines), and 150 (dashed lines); recall that the side length of the box is $L=200$. In each set of lines, the lowest line corresponds to $\theta=0$ [where $\mathbf{x}_2-\mathbf{x}_1=(z\cos\theta, z\sin\theta)$], the middle to $\theta=\pi/4$, and the highest to $\theta=\pi/2$. As expected, $S_2$ is dependent on the absolute positions of $\mathbf{x}_1$ and $\mathbf{x}_2$, not just the radial displacement.

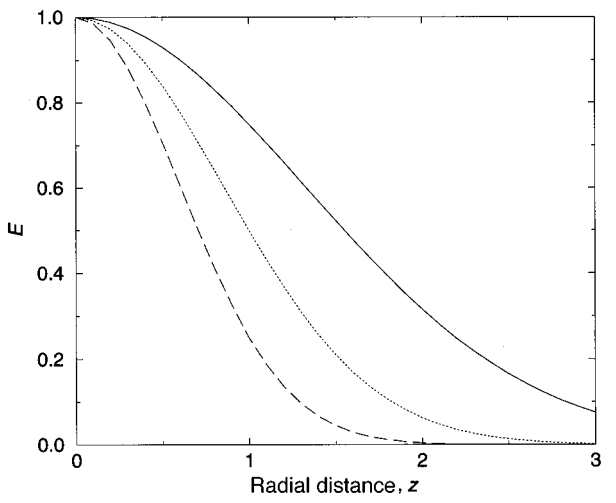


FIG. 4. Exclusion probability $E(\mathbf{x};z)$ versus radial distance $z$ for system (d) of Fig. 1. The $x$ coordinate of $\mathbf{x}$ is chosen to be 50 (solid line), 100 (dotted line), and 150 (dashed line). We see that $E$ is dependent upon the absolute position $\mathbf{x}$.

In Fig. 2, we present a graph of $S_1$ for system (d), the linear-grade model of Fig. 1. Recall that the radii of the disks is unity and the side length of the square is 200, and the origin is placed at the lower-left corner of system (d). We see that Eq. (11), obtained from Eqs. (10) and (51), is indeed very close to the true graph of $S_1$. We present graphs of $S_2$ for this same density function in Fig. 3. We see that $S_2(\mathbf{x}_1,\mathbf{x}_2)$ is dependent on both the absolute positions of $\mathbf{x}_1$ and $\mathbf{x}_2$, expressed in this figure through the location of $\mathbf{x}_1$ and the distance and direction of the displacement $\mathbf{x}_2-\mathbf{x}_1$. We also see that $S_2$ increases somewhat as $\theta$ increases from 0 to $\pi/2$ and that for $\theta \neq \pi/2$, $S_2$ decays to zero as the distance increases. This is intuitively clear since the volume fraction of phase 1 decreases as the $x$ coordinate increases.

Finally, the nearest-neighbor microstructure functions can also be obtained from the $H_n$, as given in Eqs. (36) and (37), and so

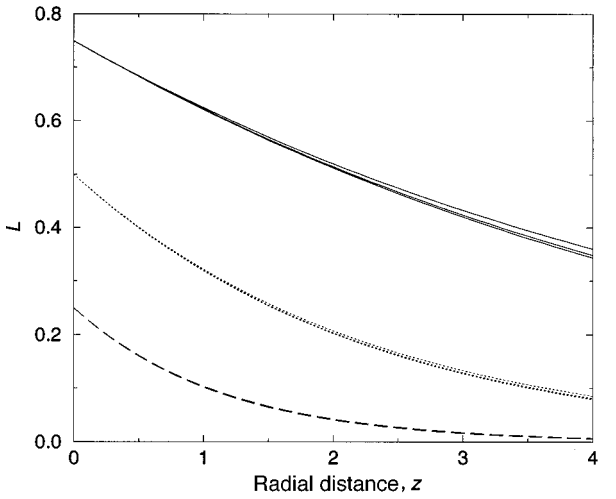


FIG. 5. Lineal-path function $L(\mathbf{x}_1,\mathbf{x}_2)$ versus radial distance $z$ for Fig. 1, calculated from Eq. (53). The legend is the same as in Fig. 3. Once again, this microstructure function is dependent on the absolute positions of $\mathbf{x}_1$ and $\mathbf{x}_2$.

$$E(\mathbf{x};z)=\exp\left[-\int_{V_1(\mathbf{x};z)}\rho(\mathbf{r})d\mathbf{r}\right] \tag{52}$$

and similarly for $H(\mathbf{x};z)$. Graphs of $E$ for the linear-grade model (d) of Fig. 1 are shown in Fig. 4.

### C. Lineal-path function

The final microstructure function analytically evaluated here is the lineal-path function $L(\mathbf{x}_1,\mathbf{x}_2)$, the probability that the line segment connecting $\mathbf{x}_1$ and $\mathbf{x}_2$ lies entirely in phase 1. This function was expressed in Sec. III simply as $L(z)$ for statistically homogeneous and isotropic two-phase random media, where $z=|\mathbf{x}_1-\mathbf{x}_2|$.

As with the $H_n$, we can substitute Eq. (40) into the series expansion (38) to obtain

$$L(\mathbf{x}_1,\mathbf{x}_2)=\exp\left[-\int_{\Omega_E(\mathbf{x}_1,\mathbf{x}_2)}\rho(\mathbf{r})d\mathbf{r}\right], \tag{53}$$

where $\Omega_E(\mathbf{x}_1,\mathbf{x}_2)$ is the region of all points within a distance $R$ of the line segment between $\mathbf{x}_1$ and $\mathbf{x}_2$.

Alternatively, this expression for $L$ can also be obtained using the properties of nonstationary Poisson process, as we now show. The line segment connecting $\mathbf{x}_1$ and $\mathbf{x}_2$ will lie entirely outside of the particles exactly when there are no particle centers in the region $\Omega_E(\mathbf{x}_1,\mathbf{x}_2)$. From Eq. (5), the probability of this event is given by Eq. (53).

In Fig. 5, we show plots of $L(\mathbf{x}_1,\mathbf{x}_2)$ for the linear-grade model (d) of Fig. 1; these plots are drawn according to the same legend as for Fig. 3. We again see that the lineal-path function is dependent on the absolute positions of its two arguments.

## V. CONCLUSION

We have proposed a microstructural model for statistically inhomogeneous random media. This model is based upon the theory of spatially nonstationary Poisson processes and can be applied to systems with any grade in volume fraction. Introducing this model of inhomogeneous fully penetrable spheres allows us to develop theoretical expressions for microstructure functions more complicated than the simple one-point microstructure function $\phi_1(\mathbf{x})$, such as the canonical $n$-point microstructure function and the lineal-path function. This quantitative characterization of the microstructure will be essential in the study of the effective properties of random media.

## ACKNOWLEDGMENTS

The authors gratefully acknowledge the support of the Office of Basic Energy Sciences of the U.S. Department of Energy under Grant No. DE-FG02-92ER14275 and the Air Force Office of Scientific Research under Grant No. F49620-92-J-0501. J.Q. acknowledges the National Science Foundation for partial financial assistance.

[1] S. Torquato and G. Stell, J. Chem. Phys. **77**, 2071 (1982).
[2] S. Torquato, J. Stat. Phys. **45**, 843 (1986).
[3] S. Torquato, Appl. Mech. Rev. **44**, 37 (1991).
[4] S. Torquato, Phys. Rev. Lett. **74**, 2156 (1995).
[5] H. L. Weissberg and S. Prager, Phys. Fluids **13**, 2958 (1970).
[6] M. Doi, J. Phys. Soc. Jpn. **40**, 567 (1976).
[7] G. W. Milton, Phys. Rev. Lett. **46**, 542 (1981).
[8] G. W. Milton and N. Phan-Thien, Proc. R. Soc. London Ser. A **380**, 305 (1982).
[9] A. K. Sen and S. Torquato, Phys. Rev. B **39**, 4504 (1989).
[10] J. Quintanilla and S. Torquato, J. Appl. Phys. **77**, 4361 (1995).
[11] L. W. Gelhar, *Stochastic Subsurface Hydrology* (Prentice-Hall, Englewood Cliffs, NJ, 1993).
[12] J. R. Bond, L. Kofman, and D. Pogosyan, Nature **380**, 603 (1996).
[13] These materials began to be studied in earnest in 1987, when Japan began a national project to develop heat-shielding structural materials for the future Japanese space program. An FGM designed for such an application would be comprised of ceramic and metal in such a way that the exterior would be entirely ceramic (for high heat resistance), the interior would be entirely metal (for high mechanical strength), and, within the material, the volume fractions of the two phases would vary between these two extremes.
[14] J. Aboudi, S. M. Arnold, and M.-J. Pindera, Compos. Eng. **4**, 1 (1994).
[15] N. Cherradi, A. Kawasaki, and M. Gasik, Compos. Eng. **4**, 883 (1994).
[16] G. J. Dvorak and J. Zuiker, in *IUTAM Symposium on Anisotropy, Inhomogeneity and Nonlinearity in Solid Mechanics*, edited by D. F. Parker and A. H. England (Kluwer Academic, Netherlands, 1995), p. 103.
[17] A. J. Markworth, K. S. Ramesh, and W. P. Parks, Jr., J. Mater. Sci. **30**, 2183 (1995).
[18] J. C. Nadeau and M. Ferrari, Compos. Eng. **5**, 821 (1995).
[19] S. Torquato, B. Lu, and J. Rubinstein, Phys. Rev. A **41**, 2059 (1990).
[20] B. Lu and S. Torquato, Phys. Rev. A **45**, 922 (1992).
[21] H. Royden, *Real Analysis*, 3rd ed. (Macmillan, New York, 1988).
[22] D. Stoyan, W. S. Kendall, and J. Mecke, *Stochastic Geometry and Its Applications*, 2nd ed. (Wiley, New York, 1995).
[23] Y. Fukui, K. Takashima, and C. B. Ponton, J. Mater. Sci. **29**, 2281 (1994).
[24] J. H. Abboud, D. R. F. West, and R. D. Rawlings, J. Mater. Sci. **29**, 3393 (1994).
[25] B. Lu and S. Torquato, Phys. Rev. A **43**, 2078 (1991).
[26] D. A. Coker, S. Torquato, and J. H. Dunsmuir, J. Geophys. Res. **100**, 17 497 (1996).
[27] M. D. Rintoul *et al.*, Phys. Rev. E **54**, 2663 (1996).
[28] E. E. Underwood, *Quantitative Stereology* (Addison-Wesley, Reading, MA, 1970).